THE JOURNAL OF BIOLOGICAL CHEMISTRY VOL. 291, NO. 14, pp. 7505–7516, April 1, 2016
© 2016 by The American Society for Biochemistry and Molecular Biology, Inc. Published in the U.S.A.

Human Neuropeptide S Receptor Is Activated via a $G\alpha_q$ Protein-biased Signaling Cascade by a Human Neuropeptide S Analog Lacking the C-terminal 10 Residues*

Received for publication, November 12, 2015, and in revised form, February 9, 2016 Published, JBC Papers in Press, February 10, 2016, DOI 10.1074/jbc.M115.704122

Yuan Liao[‡], Bin Lu[‡], Qiang Ma[‡], Gang Wu[§], Xiangru Lai[‡], Jiashu Zang[‡], Ying Shi[‡], Dongxiang Liu[¶], Feng Han[§1], and Naiming Zhou[‡2]

From the [‡]Institute of Biochemistry, College of Life Sciences, and the [§]Institute of Pharmacology and Toxicology, College of Pharmaceutical Sciences, Zijingang Campus, Zhejiang University, Hangzhou, Zhejiang 310058, China and the [¶]State Key Laboratory of Drug Research, Shanghai Institute of Materia Medica, Chinese Academy of Sciences, Shanghai 201203, China

Human neuropeptide S (NPS) and its cognate receptor regulate important biological functions in the brain and have emerged as a future therapeutic target for treatment of a variety of neurological and psychiatric diseases. The human NPS (hNPS) receptor has been shown to dually couple to $G\alpha_s$- and $G\alpha_q$-dependent signaling pathways. The human NPS analog hNPS-(1–10), lacking 10 residues from the C terminus, has been shown to stimulate Ca^{2+} mobilization in a manner comparable with full-length hNPS *in vitro* but seems to fail to induce biological activity *in vivo*. Here, results derived from a number of cell-based functional assays, including intracellular cAMP-response element (CRE)-driven luciferase activity, Ca^{2+} mobilization, and ERK1/2 phosphorylation, show that hNPS-(1–10) preferentially activates $G\alpha_q$-dependent Ca^{2+} mobilization while exhibiting less activity in triggering $G\alpha_s$-dependent CRE-driven luciferase activity. We further demonstrate that both $G\alpha_q$- and $G\alpha_s$-coupled signaling pathways contribute to full-length hNPS-mediated activation of ERK1/2, whereas hNPS-(1–10)-promoted ERK1/2 activation is completely inhibited by the $G\alpha_q$ inhibitor UBO-QIC but not by the PKA inhibitor H89. Moreover, the results of Ala-scanning mutagenesis of hNPS-(1–13) indicated that residues Lys^{11} and Lys^{12} are structurally crucial for the hNPS receptor to couple to $G\alpha_s$-dependent signaling. In conclusion, our findings demonstrate that hNPS-(1–10) is a biased agonist favoring $G\alpha_q$-dependent signaling. It may represent a valuable chemical probe for further investigation of the therapeutic potential of human NPS receptor-directed signaling *in vivo*.

Neuropeptide S (NPS),[3] with its highly conserved serine at the N-terminal residue of the mature 20-amino acid peptide, has been newly identified as an endogenous ligand for the orphan G protein-coupled receptor GPR154, hereafter referred to as the neuropeptide S receptor (NPSR) (1–3). *In situ* hybridization studies on rat brain have demonstrated that NPS expression tends to be highly localized in the distinct brain stem clusters located around the locus coeruleus. Conversely, NPSR mRNA is widely expressed within the regions of the brain involved in emotion and memory processing as well as olfaction. These include the thalamus, hypothalamus, amygdala, and cortical areas (1, 4, 5). Upon central administration in rodents, NPS has been found to exert a variety of biological effects, including reduction of anxiety-related behavior (1, 6, 7), increase of locomotor activity (6, 8, 9), stimulation of wakefulness (1, 6), inhibition of food intake (9, 10), and enhancement of memory formation (11). Recent studies have also reported its involvement in the suppression of alcohol consumption (12, 13) and in the extinction of contextual conditioned fear responses (14, 15). Thus, NPS and its cognate receptor represent a novel neurotransmitter system in CNS physiology and pathology and hold great promise for treating a variety of neurological as well as psychiatric conditions.

NPS exerts its biological actions through NPSR. Using heterologous expression systems, Chinese hamster ovary (CHO) cells, and human embryonic kidney 293 (HEK293) cells, the human and mouse NPSRs have been shown to trigger both Ca^{2+} mobilization and cAMP accumulation in response to NPS challenge. This indicates that NPSR couples to both $G\alpha_q$ and $G\alpha_s$ proteins (1, 16). Using single-cell calcium imaging in neuronal cells expressing human NPSR (hNPSR), a recent study confirmed that NPS stimulation induced a significant Ca^{2+} response via a $G\alpha_q$/phospholipase C-dependent pathway but with no involvement of the $G\alpha_s$-mediated cAMP-dependent pathway (17). In addition to intracellular Ca^{2+} mobilization and cAMP formation, NPS also stimulated extracellular signal-regulated kinase 1/2 (ERK1/2) phosphorylation through NPSR (13, 16, 18). NCGC00185684, a newly identified NPSR antagonist, was also found to preferentially block ERK phosphorylation over intracellular cAMP or calcium responses to NPS (13). However, characterization of NPS/NPSR-mediated signaling and its associated physiological functions remains in its infancy.

A structure-activity study on NPS has defined the determinant role of the N-terminal one-third, in particular residues Phe^2, Arg^3, Asn^4, and Val^6, in the involvement of NPS in the

* This work was supported by Ministry of Science and Technology of China Grants 2012CB910402 and 2012AA020303 and National Natural Science Foundation of China Grants 81173106 and 31200621. The authors declare that they have no conflicts of interest with the contents of this article.

[1] To whom correspondence may be addressed: College of Pharmaceutical Sciences, Zhejiang University, Zijingang Campus, 866 Yuhang Tang Rd., Hangzhou, 310058, China. Tel.: 86-571-88208402; Fax: 86-571-88208402; E-mail: changhuahan@zju.edu.cn.

[2] To whom correspondence may be addressed: College of Life Sciences, Zhejiang University, Zijingang Campus, 866 Yuhang Tang Rd., Hangzhou 310058, China. Tel.: 86-571-88206748; Fax: 86-571-88206134-8000; E-mail: zhounaiming@zju.edu.cn.

[3] The abbreviations used are: NPS, neuropeptide S; NPSR, NPS receptor; hNPS and hNPSR, human NPS and NPSR, respectively; GPCR, G protein-coupled receptor; CRE, cAMP-response element; HEK293, human embryonic kidney 293.

activation of NPSR (19). Based on the ability to stimulate calcium release, the fragment hNPS-(1–10) has been identified as the minimum sequence required for the activation of the human NPSR *in vitro*. However, this peptide failed to evoke a statistically significant effect *in vivo* (8). To better characterize NPS and NPSR, we established HEK293 cells expressing the hNPSR and developed several cell-based functional assays, including a CRE-based reporter gene assay, Ca^{2+} mobilization assay, and Western blotting-based ERK1/2 phosphorylation assay. To our surprise, human NPS-(1–10) was identified as a biased agonist, preferentially activating a $G\alpha_q$-dependent signaling cascade through NPSR. Further structure-activity analysis was performed to define the key residues involved in the participation of NPS in $G\alpha_q$-biased signaling.

Experimental Procedures

Materials—Dulbecco's modified Eagle's medium (DMEM) and fetal bovine serum (FBS) were purchased from Hyclone (Beijing, China). Opti-MEM® I reduced serum medium was purchased from Invitrogen. X-tremeGENE was purchased from Roche Applied Science. The pCMV-FLAG vector was purchased from Sigma. The Fura-2 acetoxymethyl ester derivative (Fura-2/AM) was purchased from Dojindo (Japan). Anti-phospho-ERK1/2 (Thr^{202}/Tyr^{204}) and anti-ERK1/2 antibodies were purchased from Cell Signaling Technology (Danvers, MA). H89 was purchased from Tocris Bioscience. UBO-QIC was purchased from E. Kostenis (University of Bonn, Bonn, Germany). The human neuropeptide S, human neuropeptide S-(1–10) (hNPS-(1–10)), human neuropeptide S-(1–13) (hNPS-(1–13)), the series of hNPS-(1–13) analogs, and Cy5-labeled hNPS (Cy5-hNPS) were synthesized by Biopeptek Biochem Ltd. (Qingdao, China).

Molecular Cloning and Plasmid Construction—The plasmid NPSR-B was purchased from Thermo. To amplify the full-length sequence encoding human NPSR, four pairs of primers were designed based on the sequence of GenBank™ entry NM_207172.1, as follows: 5′-GGGAAGCTTATGCCAGCCAACTTCACAGAGG-3′ (forward primer) and 5′-CCCTGCAGGGGAAAGAGATG-3′ (reverse primer) and 5′-ATCTCTTTCCCCTGCAGGGAGCAAAGATCACAGGATTCCAGAATGACGTTCCGGGAGAGAACTGAGAGGCATGAG-3′ (forward primer) and 5′-CCCGGATCCCTAGATGAATTCTGGCTTGGACAGAATCTGCATCTCATGCCTCTCAGTTCTCT-3′ (reverse primer) for pCMV-FLAG. The corresponding PCR products were inserted into the HindIII and BamHI sites of the pCMV-FLAG vector to produce FLAG-hNPSR. The construct was sequenced to verify the correct sequence and orientation.

Cell Culture and Transfection—The human embryonic kidney cell line (HEK293) was maintained in DMEM supplemented with 10% heat-inactivated fetal bovine serum (Hyclone) and 4 mM L-glutamine (Invitrogen). The hNPSR cDNA plasmid constructs were transfected or cotransfected into HEK293 cells using X-tremeGENE (Roche Applied Science) according to the manufacturer's instructions.

Luciferase Activity—After seeding in a 96-well plate overnight, HEK293 cells, transiently co-transfected with FLAG-hNPSR/pCRE-Luc, were grown to 90–95% confluence. The HEK293 cells were stimulated with 10 μM forskolin alone or with the indicated concentration of hNPS or hNPS-(1–10) in DMEM without FBS and then incubated for 4 h at 37 °C. Luciferase activity was detected using a firefly luciferase kit (Promega, Madison, WI). When required, the cells were treated for 1 h with or without H89 or UBO-QIC in serum-free DMEM before beginning the experiments.

Intracellular Calcium Measurement—The transiently transfected hNPSR-expressing HEK293 cells were washed once with Hanks' balanced salt solution (Dongsheng, Hangzhou, China) containing 0.025% bovine serum albumin. The cells were then loaded with 3 μM Fura-2/AM (Dojindo Molecular Technologies, Inc., Kumamoto, Japan) for 30 min at 37 °C and washed twice in Hanks' solution. They were then resuspended to 5×10^6 cells/ml in Hanks' solution. A typical experiment contained 1.0×10^6 cells/ml in each well. These cells were stimulated with the indicated concentrations of ligands. Hanks' solution was used as a negative control. The calcium flux was measured using excitation at 340 and 380 nm in a fluorescence spectrometer (Infinite F200Pro, Tecan, Männedorf, Switzerland). When required, the cells were treated for 1 h with H89 or UBO-QIC before initiation of the experiment.

ERK1/2 Activation Assay—The HEK293 cells transiently expressing FLAG-hNPSR were seeded in 24-well plates and starved for 120 min in serum-free medium to reduce background ERK1/2 activation. If required, the cells with the indicated ligand were preincubated with various inhibitors for 1 h before activation. After stimulation with the ligand, the cells were lysed in lysis buffer (20 mM HEPES (pH 7.5), 10 mM EDTA, 150 mM NaCl, 1% Triton X-100) with one tablet of complete protease inhibitor (1 tablet/50 ml; Roche Applied Science) at 4 °C for 30 min. Equal amounts of total cell lysate were size-fractionated using SDS-PAGE (10%) and then transferred to PVDF membranes (Millipore). The membranes were blocked in TBS containing 0.05% Tween 20 and 5% nonfat dry milk for 1 h at room temperature and then incubated with rabbit monoclonal anti-pERK1/2 antibody (Cell Signaling, Danvers, MA) and anti-rabbit horseradish peroxidase-conjugated secondary antibody (Beyotime, Haimen, China) according to the manufacturer's protocols. The blots were stripped and relabeled using an anti-total ERK1/2 (1:2000) monoclonal antibody as a control for protein loading. The levels of ERK1/2 phosphorylation were normalized to total ERK1/2. All of the immunoblots were quantified using a Bio-Rad Quantity One imaging system.

Binding Assay Using Cy5-labeled hNPS—A whole-cell binding assay on HEK293 cells that had been transiently transfected with human NPSR was performed as described previously (20, 21). In brief, HEK293 cells expressing hNPSR were detached using non-enzyme cell dissociation buffer and, after washing twice with 1 ml of ice-cold PBS, were resuspended in binding buffer (Hanks' balanced salt solution containing 0.025% bovine serum albumin). Binding experiments were performed in a final volume of 200 μl of binding buffer containing 5×10^5 cells and incubated with 100 nM Cy5-labeled hNPS in the absence or presence of different concentrations of unlabeled NPS at room temperature for 60 min. Cells were then washed three times with 500 μl of ice-

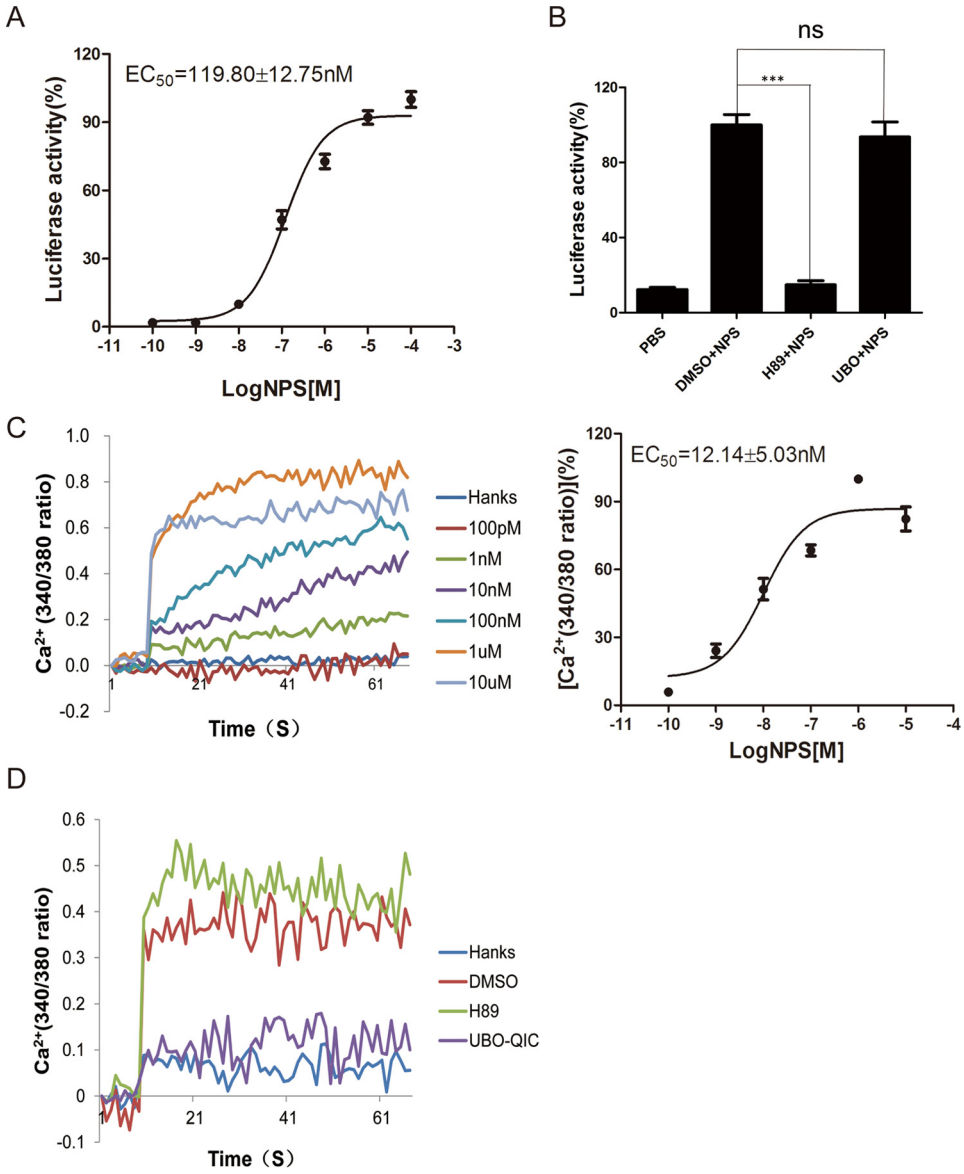

FIGURE 1. **hNPS-mediated CRE-driven luciferase activity and Ca^{2+} mobilization in NPSR-expressing HEK293 cells.** *A*, CRE-driven luciferase activity in HEK293 cells transiently co-transfected with CRE-Luc and NPSR was determined in response to different doses of hNPS. *B*, effects of different inhibitors on CRE-driven luciferase activity. HEK293 cells were pretreated with a PKA inhibitor (H89, 10 μM) and Gα_q inhibitor (UBO-QIC, 100 nM) for 1 h prior to incubation with hNPS (1 μM) for 4 h. *C*, HEK293 cells transiently transfected with NPSR were measured in response to different concentrations of hNPS using the fluorescent Ca^{2+} indicator Fura-2. *D*, effects of pretreatment of the Gα_q inhibitor (UBO-QIC, 100 nM) and the PKA inhibitor (H89, 10 μM) on hNPS-mediated Ca^{2+} influx in HEK293 cells. Data were analyzed by using Student's *t* test (***, $p < 0.001$; ns, not significant). All pictures and data shown represent the means ± S.E. (*error bars*) from at least three independent experiments.

cold standard solution with 0.1% BSA and determined by measuring the fluorescence intensity with a flow cytometer (Beckman Coulter). Binding is presented as a percentage of the NPS binding.

Bias Calculation and Data Analysis—The bias of hNPS analogs for Gα_q engagement *versus* Gα_s was determined by analyzing the concentration-response curves using the operational model as described previously (22–24). To quantify the ligand bias, log*R* (equivalent to log(τ/*KA*), the logarithm of the "transduction coefficient") was deduced from the dose-response curves fitted using the operational model-partial agonist function by GraphPad Prism version 6 with the following equation (25),

$$\text{Response} = \text{basal} + \frac{(E_m - \text{basal})}{1 + \left[\frac{\left(\frac{[A]}{10^{\log KA}} + 1\right)}{10^{\log \frac{\tau}{KA}} \times [A]}\right]^n} \quad \text{(Eq. 1)}$$

where basal is the background level of response in the absence of agonist, E_m is the maximal effect of the system, [*A*] is the molar concentration of ligand, *KA* is the functional equilibrium dissociation constant of the ligand, *n* is the slope of the transducer function linking occupancy to response, and τ is an index of the ligand efficacy in the operational model. To calculate the $\Delta\log(\tau/KA)$, which represents the relative ability of hNPS to activate a given signaling pathway, taking hNPS-(1–10) as an

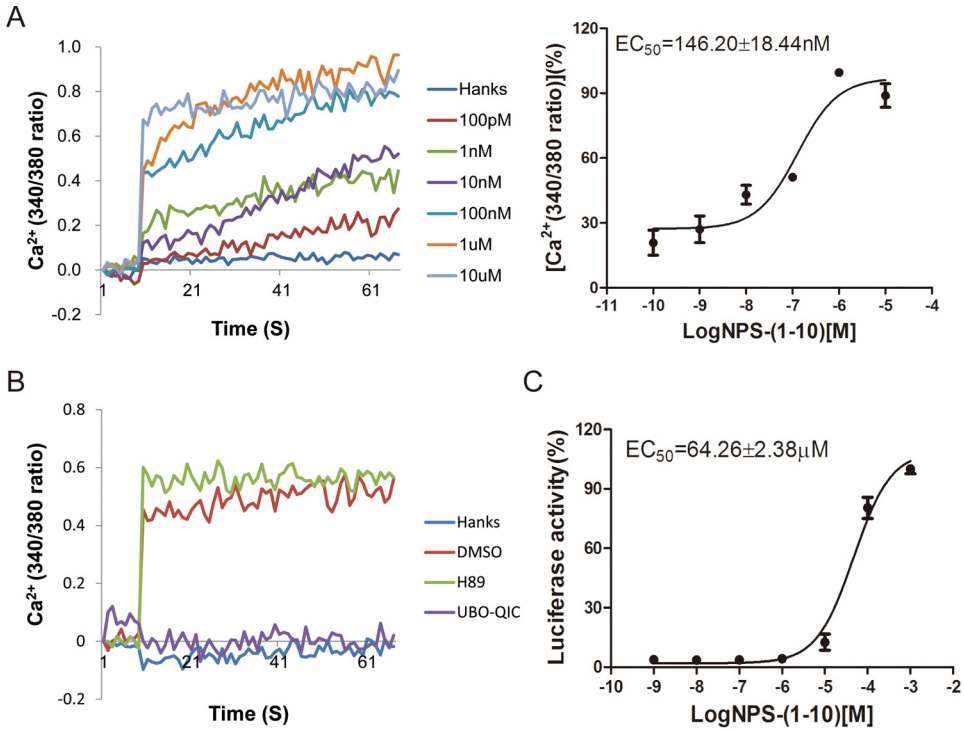

FIGURE 2. **hNPS-(1–10)-mediated CRE-driven luciferase activity and Ca^{2+} mobilization in NPSR-expressing HEK293 cells.** *A*, HEK293 cells transiently transfected with NPSR were measured in response to different concentrations of hNPS-(1–10) using the fluorescent Ca^{2+} indicator Fura-2. *B*, effects of pretreatment with the $G\alpha_q$ inhibitor (UBO-QIC, 100 nM) on hNPS-(1–10)-mediated Ca^{2+} influx in HEK293 cells. *C*, CRE-driven luciferase activity in HEK293 cells transiently co-transfected with CRE-Luc and NPSR was determined in response to different doses of hNPS-(1–10). All pictures and data shown represent the means ± S.E. (*error bars*) from at least three independent experiments.

example, we determined the log(τ/KA) values for each pathway and subtracted the log(τ/KA) for hNPS-(1–10) from the log(τ/KA) for hNPS using the following equation.

$$\Delta \text{LogR}_{\text{NPS-(1–10):cAMP}} = \text{logR}_{\text{NPS-(1–10):cAMP}} - \text{logR}_{\text{NPS:cAMP}} \quad \text{(Eq. 2)}$$

To determine the ΔΔlog(τ/KA), which represents the relative activity of hNPS analogs for a pathway over another as compared with wild-type hNPS, we calculate ΔΔlog$R$ ratios using the following equation.

$$\Delta\Delta \text{LogR}_{\text{NPS-(1–10):G}\alpha_q-\text{G}\alpha_s} = \Delta \text{logR}_{\text{NPS-(1–10):G}\alpha_q} - \Delta \text{logR}_{\text{NPS-(1–10):G}\alpha_s} \quad \text{(Eq. 3)}$$

Finally, the bias factor (BF) was calculated by determining the inverse log of the ΔΔlog$R$ ratios.

$$\text{BF}_{\text{NPS-(1–10):G}\alpha_q-\text{G}\alpha_s} = 10^{\Delta\Delta \text{logR}} \quad \text{(Eq. 4)}$$

All results are expressed as the mean ± S.E. Data were analyzed using nonlinear curve fitting (GraphPad Prism version 6.0) to obtain EC_{50} values. Statistical significance was determined using Student's t test. Probability values that were ≤0.05 were considered significant.

Results

NPSR Is Dually Coupled to Gα$_s$- and Gα$_q$-dependent Signaling Pathways—To fully characterize the human NPS and the fragment NPS-(1–10), functional assays, including the CRE-driven reporter-based cAMP accumulation assay, Fura-2-based Ca^{2+} mobilization assay, and Western blotting-based ERK1/2 phosphorylation assay, were developed using HEK293 cells transfected with the human NPS receptor. As shown in Fig. 1*A*, the administration of NPS stimulated a significant increase of luciferase activity in HEK293 cells co-transfected with the NPS receptor and a construct consisting of the firefly luciferase coding region under the control of a minimal promoter containing CREs with EC_{50} values of 119.80 ± 12.75 nM. We next sought to assess the detailed hNPSR-mediated signaling pathways with different specific inhibitors. Pretreatment of cells with H89, an inhibitor of PKA, led to a large decrease of hNPS-stimulated CRE-driven luciferase activity. However, co-incubation with UBO-QIC, a compound analogous to YM-254890 (26), which inhibits $G\alpha_q$ protein, resulted in no inhibitory effect on CRE-driven luciferase activity (Fig. 1*B*). This suggests that $G\alpha_s$ protein, but not $G\alpha_q$ protein, is involved in the NPSR-mediated cAMP/PKA signaling pathway.

In addition to the cAMP response, hNPS has also been reported to induce Ca^{2+} mobilization (1). Thus, we next examined the role of $G\alpha_q$ protein in hNPSR-mediated signaling pathways using the calcium-sensitive probe Fura-2. As indicated in Fig. 1*C*, upon activation by NPS, the hNPSR induced a rapid transient rise of intracellular Ca^{2+} mobilization with an EC_{50} value of 12.14 ± 5.03 nM. Preincubation of cells with 100 nM UBO-QIC led to a significant decrease in intracellular Ca^{2+} mobilization. In contrast, treatment with H89 showed no inhibitory effect on Ca^{2+} mobilization. This suggests that hNPSR-mediated Ca^{2+} mobilization is $G\alpha_q$-dependent and $G\alpha_s$-independent. Taken together, these data demonstrate that hNPSR dually couples to $G\alpha_s$ and $G\alpha_q$ proteins, triggering adenylate

cyclase/cAMP/PKA and phospholipase C/Ca^{2+}/PKC signaling cascades, respectively.

hNPS-(1–10) Exhibits Preferential Activity in Gα$_q$-coupled Signaling Pathway over Gα$_s$-dependent Cascade through NPSR—It has been reported that the fragment hNPS-(1–10) is able to activate hNPSR, inducing intracellular Ca^{2+} mobilization (8, 19). We next used our functional assays to define the pharmacological characteristics of hNPS-(1–10). As shown in Fig. 2*A*, the hNPSR induced a concentration-dependent elevation in intracellular Ca^{2+} in a UBO-QIC-sensitive but H89-insensitive manner with an EC_{50} value of 146.20 ± 18.44 nM in response to the hNPS-(1–10) challenge. Our data show that hNPS-(1–10) was 10-fold less potent compared with full-length NPS. This observation is comparable with the observation by Bernier *et al.* (19) but somewhat contradictory to the results obtained by Roth *et al.* (8). Moreover, we also examined whether hNPS-(1–10) can activate the Gα$_s$-coupled cAMP/PKA signaling pathway. The challenge of hNPS-(1–10) induced an increase in luciferase activity but with significantly less potency as compared with wild type NPS, having an EC_{50} value of 64.26 ± 2.38 μM. Our data indicate that there are interesting differences in agonist activity for hNPS-(1–10) between Gα$_q$ and Gα$_s$ coupling. Therefore, we next performed a quantitative analysis of hNPS-(1–10) bias based on functional parameters using an operational model as described previously (25, 27, 28). As shown in Table 1, hNPS-(1–10) activation of NPSR revealed a significant bias (>80-fold) for Gα$_q$ activation over Gα$_s$.

hNPS-(1–10) Displays the Ability to Bind to the NPSR to the Same Extent as Full-length NPS—To assess the direct interaction of both hNPS and hNPS-(1–10) with hNPSR, we designed and synthesized hNPS conjugated with the fluorescent dye Cy5 at Lys^{19} (Cy5-[Lys^{19}]hNPS). Analysis using a CRE-driven luciferase assay demonstrated that the Cy5-[Lys^{19}]hNPS peptide could activate hNPSR, leading to a dose-dependent increase in luciferase activity, with an EC_{50} value of 1.50 μM in HEK293 cells (Fig. 3*A*). Competitive binding analysis using Cy5-[Lys^{19}]hNPS, combined with FACS analysis, was performed on HEK293 cells expressing the human NPS receptor as well as with untransfected HEK293 cells as a control. As shown in Fig. 3*B*, hNPS-(1–10) exhibited the same potential to displace the binding of Cy5-[Lys^{19}]hNPS to hNPSR, comparable with that of hNPS in hNPSR-expressing HEK293 cells. However, hNPS showed no activity in disreplacement of the binding of Cy5-labeled-hNPS in hNPSR-untransfected HEK293 cells (data not shown). This suggests that deletion of the C-terminal 10 residues shows no significant effect on NPS binding to NPSR.

hNPS Induces Gα$_q$- and Gα$_s$-dependent ERK1/2 Activation, whereas hNPS-(1–10) Triggers Gα$_q$-dependent ERK1/2 Phosphorylation—ERK1/2 activation is often used as a general marker of convergent activation of multiple pathways, including both G protein-dependent and G protein-independent pathways (29). We next investigated hNPS and hNPS-(1–10)-mediated activation of ERK1/2 using a phospho-specific antibody that binds only to the phosphorylated (Thr^{202} and Tyr^{204} of ERK1 and Thr^{185} and Tyr^{187} of ERK2) forms of these kinases (30). As revealed in Fig. 4, *A–D*, treatment of cells with hNPS or hNPS-(1–10) elicited transient phosphorylation of ERK1/2 with maximal phosphorylation evident at 5 min, which returned to nearly basal levels by 60 min. Dose-response analysis showed that hNPS and hNPS-(1–10) could induce a concentration-dependent activation of ERK1/2 with EC_{50} values of 15.20 ± 5.31 and 524.60 ± 29.40 nM, respectively. Furthermore, we used different inhibitors to determine the role of Gα$_q$ and Gα$_s$ in hNPS- and hNPS-(1–10)-mediated activation of the ERK1/2 signaling pathway. Our results demonstrated that the hNPS-induced ERK1/2 phosphorylation was attenuated by both Gα$_q$ inhibitor UBO-QIC and PKA inhibitor H89 (Fig. 4, *E* and *F*). However, only the Gα$_q$ inhibitor but not the PKA inhibitor exhibited an inhibitory effect on hNPS-(1–10)-mediated activation of ERK1/2 (Fig. 4, *G* and *H*). Altogether, these results suggest that the full-length hNPS activates the ERK1/2 signaling pathway via Gα$_q$- and Gα$_s$-coupled cascades, whereas the

TABLE 1
ΔΔLog(*τ*/*KA*) ratios and bias factors for hNPS and hNPS-(1–10)

Peptide	Log(*τ*/*KA*)	ΔLog(*τ*/*KA*)	ΔΔLog(*τ*/*KA*)	Bias factor
Gα$_{s\ activation}$				
NPS	6.76 ± 0.19	0.00 ± 0.27		
NPS-(1–10)	4.34 ± 0.02	−2.42 ± 0.19		
Gα$_{q\ activation}$				
NPS	7.60 ± 0.20	0.00 ± 0.28	0.00 ± 0.39	1.00
NPS-(1–10)	7.09 ± 0.04	−0.51 ± 0.20	1.91 ± 0.48	81.28

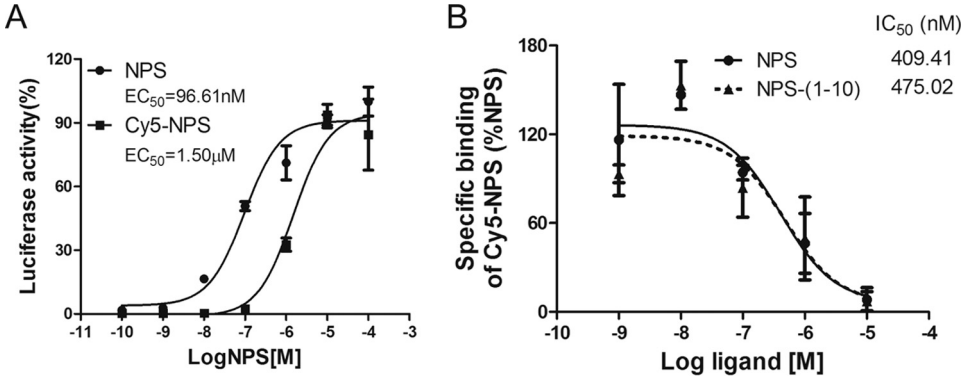

FIGURE 3. **Direct interaction of NPSR with hNPS and hNPS-(1–10).** *A*, Cy5-[Lys^{19}]NPS activity was assayed using the CRE-driven luciferase system. *B*, binding of 100 nM Cy5-[Lys^{19}]NPS, in the presence or absence of different concentrations of unlabeled hNPS and hNPS-(1–10), was determined on hNPSR-transfected and untransfected cells. The extent of binding was determined by fluorescence intensity. Nonspecific binding was determined by detecting Cy5-NPS binding in the presence of 10 μM unlabeled NPS, whereas specific binding was calculated by subtracting nonspecific binding from the total. The data shown are presented as a percentage of hNPS binding and are representative of at least three independent experiments.

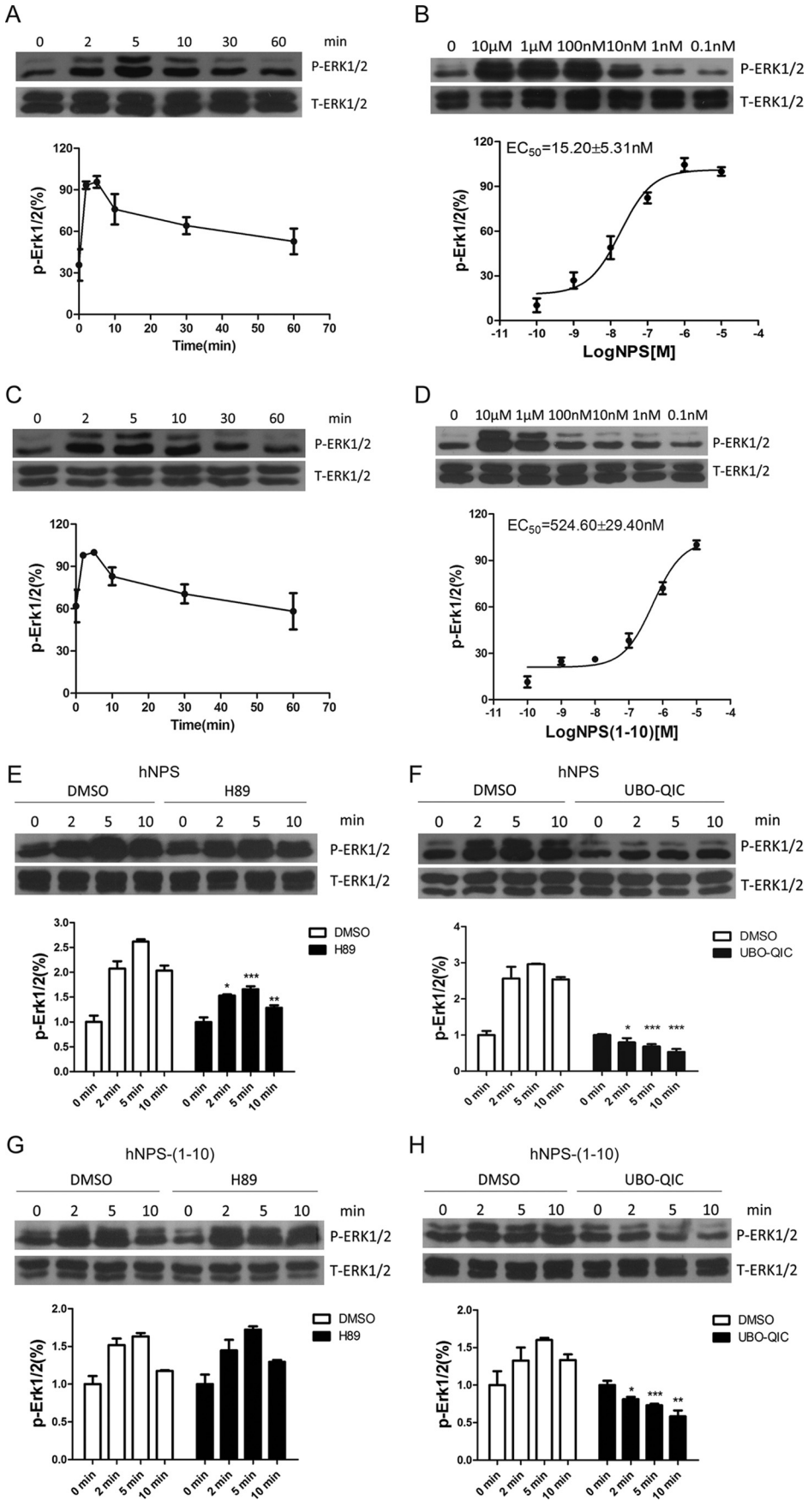
A
0 2 5 10 30 60 min
P-ERK1/2
T-ERK1/2
p-Erk1/2(%)
Time(min)
B
0 10μM 1μM 100nM 10nM 1nM 0.1nM
P-ERK1/2
T-ERK1/2
EC50=15.20±5.31nM
p-Erk1/2(%)
LogNPS[M]
C
0 2 5 10 30 60 min
P-ERK1/2
T-ERK1/2
p-Erk1/2(%)
Time(min)
D
0 10μM 1μM 100nM 10nM 1nM 0.1nM
P-ERK1/2
T-ERK1/2
EC50=524.60±29.40nM
p-Erk1/2(%)
LogNPS(1-10)[M]
E
hNPS
DMSO
H89
0 2 5 10 0 2 5 10 min
P-ERK1/2
T-ERK1/2
p-Erk1/2(%)
DMSO
H89
0 min 2 min 5 min 10 min
F
hNPS
DMSO
UBO-QIC
0 2 5 10 0 2 5 10 min
P-ERK1/2
T-ERK1/2
p-Erk1/2(%)
DMSO
UBO-QIC
0 min 2 min 5 min 10 min
G
hNPS-(1-10)
DMSO
H89
0 2 5 10 0 2 5 10 min
P-ERK1/2
T-ERK1/2
p-Erk1/2(%)
DMSO
H89
0 min 2 min 5 min 10 min
H
hNPS-(1-10)
DMSO
UBO-QIC
0 2 5 10 0 2 5 10 min
P-ERK1/2
T-ERK1/2
p-Erk1/2(%)
DMSO
UBO-QIC
0 min 2 min 5 min 10 min

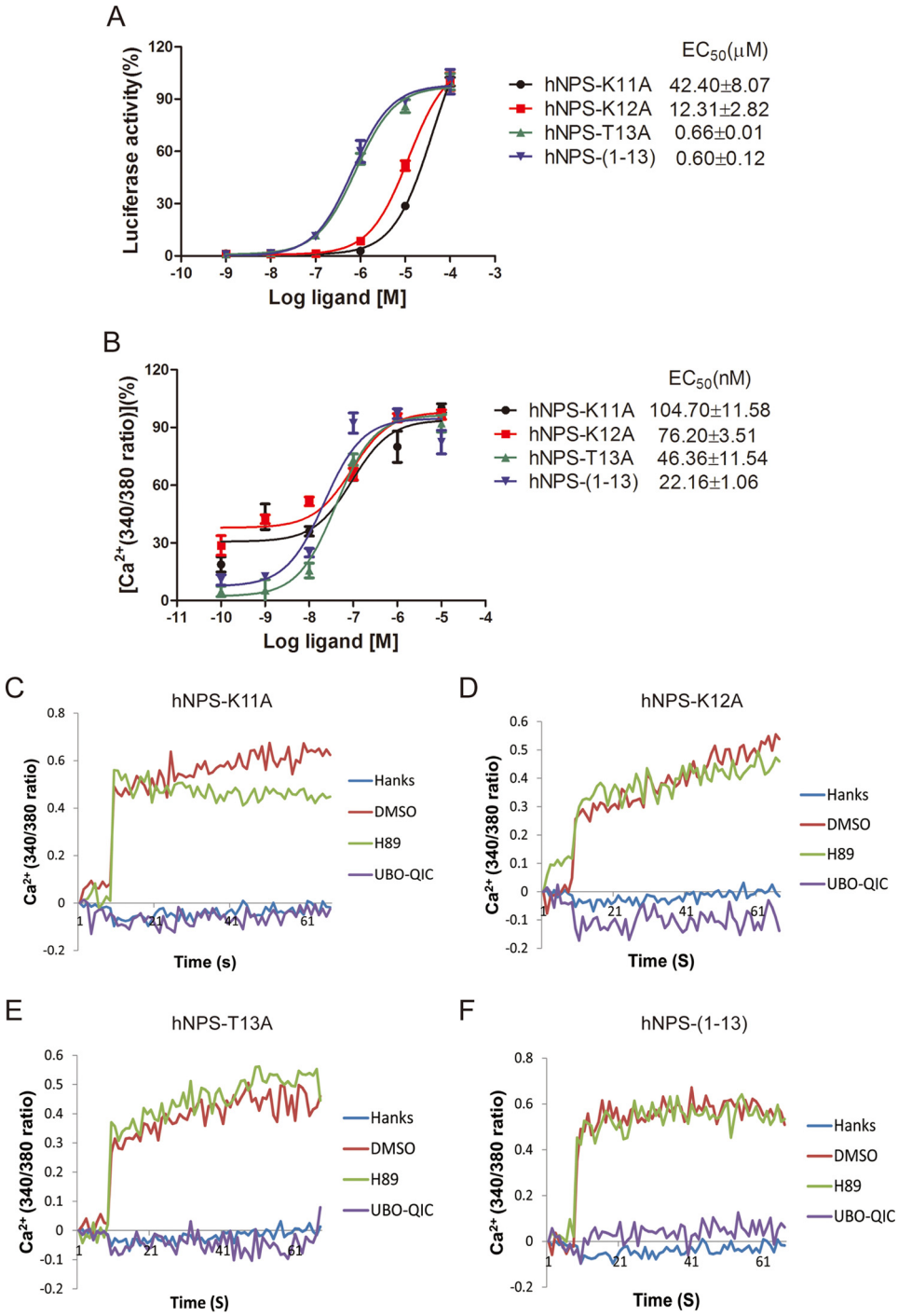

FIGURE 5. **The hNPS-(1–13) analogs-mediated CRE-driven luciferase activity and Ca^{2+} mobilization in NPSR-expressing HEK293 cells.** *A*, CRE-driven luciferase activity in HEK293 cells transiently co-transfected with CRE-Luc and NPSR was determined in response to different doses of hNPS. *B*, HEK293 cells transiently transfected with NPSR were measured in response to different concentrations of the hNPS-(1–13) analogs using the fluorescent Ca^{2+} indicator Fura-2. Effects of pretreatment of $G\alpha_q$ inhibitor (UBO-QIC, 100 nM) on the hNPS-(1–13) analog-mediated Ca^{2+} influx in HEK293 cells (*C–F*). All pictures and data shown represent the means ± S.E. (*error bars*) from at least three independent experiments. *P-ERK*, phospho-ERK; *T-ERK*, total ERK.

FIGURE 4. **NPSR activates ERK1/2 mainly via $G\alpha_q$-dependent signaling pathway by hNPS and hNPS-(1–10) in HEK293 cells.** *A* and *B*, time course (*A*) and concentration dependence (*B*) of hNPS-stimulated phosphorylation of ERK1/2 in HEK293 cells transiently transfected with NPSR. *C* and *D*, time course (*C*) and concentration dependence (*D*) of hNPS-(1–10)-stimulated phosphorylation of ERK1/2 in HEK293 cells transiently transfected with NPSR. *E* and *F*, time course of PKA inhibitor H89 (10 μM) (*E*) and $G\alpha_q$ inhibitor UBO-QIC (100 nM) (*F*) on hNPS-mediated activation of ERK1/2. *G* and *H*, time course of PKA inhibitor H89 (10 μM) (*G*) and $G\alpha_q$ inhibitor UBO-QIC (100 nM) (*H*) on hNPS-(1–10)-mediated activation of ERK1/2. The cells were pretreated with or without (control) inhibitors for 1 h and then stimulated with hNPS or hNPS-(1–10) (1 μM, 5 min). The phospho-ERK (*P-ERK*) was normalized to a loading control (total ERK (*T-ERK*)). All pictures and data shown represent the means ± S.E. (*error bars*) from at least three independent experiments. Statistical analysis was performed by a two-tailed Student's *t* test (*, $p < 0.05$; **, $p < 0.01$; ***, $p < 0.001$, *versus* counterpart control).

TABLE 2
ΔΔLog(*τ*/*KA*) ratios and bias factors for hNPS-(1–13) analogs

Peptide	Log(*τ*/*KA*)	ΔLog(*τ*/*KA*)	ΔΔLog(*τ*/*KA*)	Bias factor
Gα$_{s\ activation}$				
NPS	6.76 ± 0.19	0.00 ± 0.27		
NPS-K11A	4.74 ± 0.02	−2.02 ± 0.19		
NPS-K12A	5.39 ± 0.05	−1.37 ± 0.20		
NPS-T13A	6.32 ± 0.11	−0.44 ± 0.22		
NPS-(1–13)	6.37 ± 0.10	−0.39 ± 0.21		
Gα$_{q\ activation}$				
NPS	7.60 ± 0.20	0.00 ± 0.28	0.00 ± 0.39	1.00
NPS-K11A	7.42 ± 0.04	−0.18 ± 0.20	1.84 ± 0.28	69.18
NPS-K12A	7.44 ± 0.35	−0.16 ± 0.40	1.21 ± 0.45	16.22
NPS-T13A	7.56 ± 0.05	−0.04 ± 0.21	0.40 ± 0.30	2.51
NPS-(1–13)	7.55 ± 0.31	−0.05 ± 0.37	0.34 ± 0.43	2.19

hNPS-(1–10) fragment induces ERK1/2 phosphorylation through a Gα$_q$-dependent pathway.

Involvement of Key Residues in the hNPS-mediated Activation of Gα$_s$-dependent Signaling (Molecular Basis for NPS Coupling Selectivity)—To investigate the role of specific amino acid residues within NPS, alanine-scanning mutagenesis was performed to assess the effect of these mutants on NPSR activation. hNPS-(1–13) has been shown to activate the human NPS receptor with a maximum effect and potency comparable with wild type NPS (8, 19). Our data, derived from a functional assay using a combination of specific inhibitors, showed that hNPS-(1–13) was able to stimulate CRE-driven luciferase activity and Ca^{2+} mobilization in a UBO-QIC- and H89-sensitive manner. This suggests the involvement of both Gα$_q$ and Gα$_s$ proteins in the hNPS-(1–13)-induced signaling cascades. Altogether, these results narrow down the key residues involved in the NPS-mediated activation of the Gα$_s$-coupled signaling pathway to three residues: Lys^{11}, Lys^{12}, and Thr^{13}. Thus, we synthesized three alanine-substituted hNPS-(1–13) analogs for further evaluation of possible contributions of these amino acids to the activation of the NPS-mediated Gα$_s$-coupled signaling pathway. As shown in Fig. 5 (*A* and *B*) and Table 2 with the human NPS receptor, peptides hNPS-T13A and hNPS-(1–13) showed the same ability to induce Gα$_q$- and Gα$_s$-coupled signaling pathways, whereas hNPS-K11A and hNPS-K12A exhibited a significant bias (≥69- and ≥16-fold, respectively) for Gα$_q$ activation over Gα$_s$.

Preincubation of cells with 100 nM UBO-QIC led to a significant decrease in the intracellular Ca^{2+} mobilization for both alanine-substituted hNPS-(1–13) analogs. In contrast, treatment with H89 showed no inhibitory effect on Ca^{2+} mobilization, suggesting that Ca^{2+} mobilization is Gα$_q$-dependent and Gα$_s$-independent for all alanine-substituted hNPS-(1–13) analogs. Taken together, it is likely that residues Lys^{11} and Lys^{12} play critical roles in the human NPS-mediated Gα$_s$-coupled signaling pathway.

The hNPS-(1–13) Analog Induces ERK1/2 Activation Triggered by Different Signaling Pathways—As mentioned above, hNPS-T13A and hNPS-(1–13) showed the same ability to induce Gα$_q$- and Gα$_s$-coupled signaling pathways, whereas hNPS-K11A and hNPS-K12A exhibited a significant bias for Gα$_q$ activation over Gα$_s$. Western blotting was then used to confirm the role of Gα$_q$ and Gα$_s$ in the hNPS-(1–13) analog-induced activation of ERK1/2. As shown in Fig. 6, hNPS-K11A and hNPS-K12A-mediated ERK1/2 phosphorylation was suppressed by the Gα$_q$ inhibitor UBO-QIC but not by the PKA inhibitor H89 (Fig. 6, *A–D*), whereas hNPS-T13A and hNPS-(1–13)-induced activation of ERK1/2 was not only blocked by UBO-QIC but also inhibited by H89. Taken together, these results confirm that Lys^{11} and Lys^{12} play a critical role in human NPS-mediated Gα$_s$-coupled signaling.

Discussion

It has been previously established that the NPS receptor is dually coupled to Gα$_s$ and Gα$_q$-proteins and that activation by NPS leads to a rapid and transient increase in intracellular cAMP and Ca^{2+} (1, 13, 16–18, 31, 32). Upon agonist stimulation, the NPSR also signals to the ERK1/2 signaling pathway (13, 16, 18), although the exact mechanisms linking the cross-talk of NPSR to ERK1/2 remain unknown. Thus, we used HEK293 cells, transiently transfected with the NPS receptor, to develop a Ca^{2+} mobilization assay, CRE-luciferase-based cAMP assay, and ERK1/2 phosphorylation assay for functional characterization of NPS and NPSR. Our data demonstrate that NPS induces a significant rise of intracellular Ca^{2+} with an EC_{50} value of 12.14 ± 5.03 nM that is sensitive to the novel Gα$_q$-dependent inhibitor UBO-QIC (33) but insensitive to the PKA inhibitor H89. However, treatment of cells with NPS resulted in an increase of luciferase activity with an EC_{50} value of 119.80 ± 12.75 nM in a H89-sensitive and UBO-QIC-insensitive manner. This suggests that the NPS receptor dually activates Gα$_q$- and Gα$_s$-coupled cascades. However, the NPS-mediated activation of ERK1/2 signaling was both Gα$_q$- and Gα$_s$-dependent. ERK1/2 activation is often used as a general marker of the convergent activation of multiple pathways (29). With a broader range of functional assays, the ERK1/2 pathway has been suggested to be a better assay for full evaluation of the potential of ligand-directed signaling and functional selectivity (34).

We next evaluated hNPS-(1–10)-mediated signaling across three pathways. These were Gα$_s$-dependent CRE-driven luciferase activity, Gα$_q$-dependent Ca^{2+} mobilization, and Gα$_s$- and Gα$_q$-dually coupled ERK1/2 activation. Surprisingly, we observed that the hNPS-(1–10)-mediated activation of the NPS receptor induced signaling biased toward the Gα$_q$-dependent pathway (Ca^{2+} mobilization EC_{50} = 146.20 ± 18.44 nM) over the Gα$_s$-coupled pathway (CRE-driven luciferase activity EC_{50} = 64.26 ± 2.38 μM) with a biased value of 81.3. This bias provided clear evidence that the hNPS-(1–10)-induced ERK1/2 phosphorylation had been attenuated by the Gα$_q$ inhibitor UBO-QIC but not by the PKA inhibitor H89. Binding analysis using fluorescence-labeled NPS showed a similar activity in binding with the NPS receptor between WT NPS and NPS-(1–10). These data strongly suggest that the fragment hNPS-(1–10) activates signaling biased toward the Gα$_q$-coupled cascade over Gα$_s$-dependent cascade through the NPS receptor. A previous report had observed that the N-terminal sequence 1–10 of human NPS showed similar potencies and efficacies as full-length NPS, but this conclusion was only based on the data derived from Ca^{2+} mobilization assays (8).

It is now generally accepted that at GPCRs, different ligands exist that preferentially activate one signaling pathway over another. This process has been termed biased signaling or functional selectivity (35–37). Biased activation of signaling path-

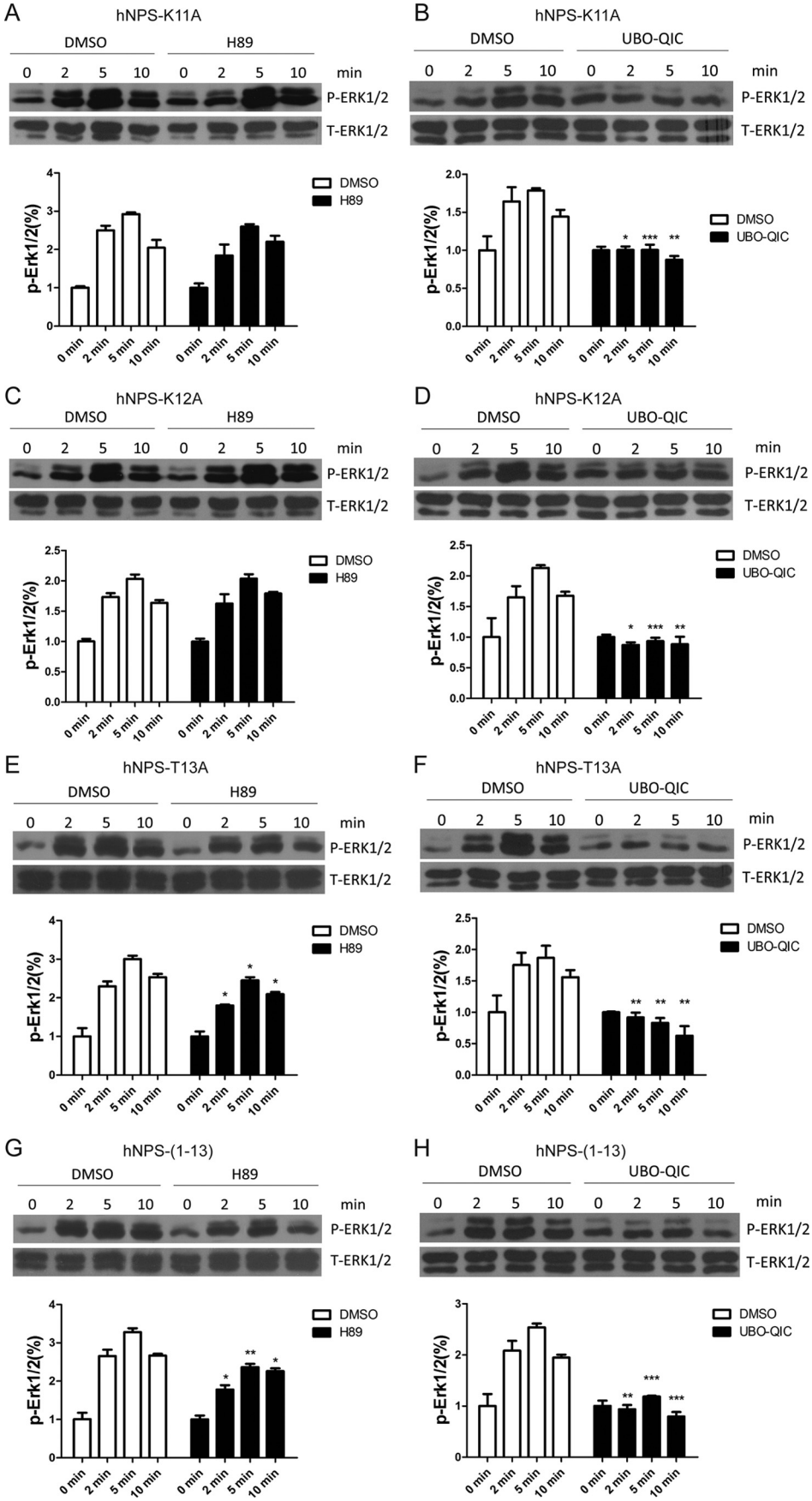
A
hNPS-K11A
DMSO
H89
0 2 5 10 0 2 5 10 min
P-ERK1/2
T-ERK1/2
p-Erk1/2(%)
DMSO
H89
0 min 2 min 5 min 10 min 0 min 2 min 5 min 10 min
B
hNPS-K11A
DMSO
UBO-QIC
0 2 5 10 0 2 5 10 min
P-ERK1/2
T-ERK1/2
p-Erk1/2(%)
DMSO
UBO-QIC
* *** **
0 min 2 min 5 min 10 min 0 min 2 min 5 min 10 min
C
hNPS-K12A
DMSO
H89
0 2 5 10 0 2 5 10 min
P-ERK1/2
T-ERK1/2
p-Erk1/2(%)
DMSO
H89
0 min 2 min 5 min 10 min 0 min 2 min 5 min 10 min
D
hNPS-K12A
DMSO
UBO-QIC
0 2 5 10 0 2 5 10 min
P-ERK1/2
T-ERK1/2
p-Erk1/2(%)
DMSO
UBO-QIC
* *** **
0 min 2 min 5 min 10 min 0 min 2 min 5 min 10 min
E
hNPS-T13A
DMSO
H89
0 2 5 10 0 2 5 10 min
P-ERK1/2
T-ERK1/2
p-Erk1/2(%)
DMSO
H89
* * *
0 min 2 min 5 min 10 min 0 min 2 min 5 min 10 min
F
hNPS-T13A
DMSO
UBO-QIC
0 2 5 10 0 2 5 10 min
P-ERK1/2
T-ERK1/2
p-Erk1/2(%)
DMSO
UBO-QIC
** ** **
0 min 2 min 5 min 10 min 0 min 2 min 5 min 10 min
G
hNPS-(1-13)
DMSO
H89
0 2 5 10 0 2 5 10 min
P-ERK1/2
T-ERK1/2
p-Erk1/2(%)
DMSO
H89
* ** *
0 min 2 min 5 min 10 min 0 min 2 min 5 min 10 min
H
hNPS-(1-13)
DMSO
UBO-QIC
0 2 5 10 0 2 5 10 min
P-ERK1/2
T-ERK1/2
p-Erk1/2(%)
DMSO
UBO-QIC
** *** ***
0 min 2 min 5 min 10 min 0 min 2 min 5 min 10 min

ways by specific ligands has been documented for several other GPCRs, including dopamine D2R (38), the apelin receptor APJ (28), the ghrelin receptor GSHR1a (38), the type 1 parathyroid hormone receptor (39–41), the urotensin II receptor (42), the V2 vasopressin receptor (43), the human free fatty acid receptor GPR120 (44), and the prokineticin receptor 2 (45). However, most GPCRs whose biased signaling has been investigated have exhibited bias between G protein- and arrestin-dependent pathways. Recent studies provide evidence that in some GPCRs, such as in the chemokine receptors (46), the calcium-sensing receptor (47, 48), the histamine H2 receptor (49), the human oxytocin receptor (50), the prokineticin receptor 2 (45), and the follicle-stimulating hormone receptor (51), biased agonism also activates selective G protein pathways. Here, we provide another example of a GPCR signaling bias toward the Gα$_q$-dependent pathway over Gα$_s$-coupled pathway. Our recent study has demonstrated that the *Drosophila melanogaster* sex peptide (DmSP) binds to the *Bombyx* prothoracicostatic peptide receptor at an allosteric site. This leads to a Gα$_{i/o}$-protein-biased signaling pathway without any interference with Ca^{2+} mobilization and β-arrestin recruitment (20). K16P, an apelin fragment lacking the C-terminal phenylalanine, has been also observed to orthosterically activate biased signaling favoring the Gα$_i$-dependent over the β-arrestin-dependent pathway (28). The structure-activity studies of the M2 muscarinic acetylcholine receptor revealed that single-point mutations both in the orthosteric (Y104$^{3.33}$A) and allosteric (Y177A) sites were identified to selectively affect signaling pathway-selective effects (34). Collectively, it is more likely that the peptide NPS-(1–10) binds to the orthosteric site of the NPS receptor, leading to the activation of biased signaling favoring Gα$_q$- over Gα$_s$-coupled pathways.

Studies of structure-activity relationships for NPS have suggested that the first residues, in particular Phe^2, Arg^3, and Asn^4, are necessary and sufficient for the activation of NPSR (8, 19). Despite the N-terminal sequence NPS-(1–10) being found to produce a similar maximum effect and potency as the reference peptide NPS-(1–20) in Roth *et al.* (8), our data showed that NPS-(1–10) was 10-fold less potent as compared with wild type NPS, whereas NPS-(1–13) exhibited similar activities in the stimulation of CRE-driven luciferase activity and Ca^{2+} mobilization comparable with the full-length NPS peptide. Our observation was consistent with that of Bernier *et al.* (19). The reason for the discrepancy between our results and those of Bernier *et al.* (19) as compared with those of Roth *et al.* (8) is unknown, but it is probably linked to different assay systems and cell lines used in the studies. Our further analysis demonstrated that NPS-(1–13)-mediated ERK1/2 phosphorylation was sensitive to treatment of the Gα$_q$ inhibitor UBO-QIC and the PKA inhibitor H89. This implies that at the NPSR, NPS-(1–13) induces both Gα$_q$- and Gα$_s$-dependent signaling pathways. To investigate the role of specific amino acid residues with NPS, we performed site-directed mutagenesis of the peptide and assessed the effect of these mutants on NPSR activation. Our results indicated that the substitution of Lys^{11} and Lys^{12} with alanine largely resulted in the inactivation of Gα$_s$-dependent CRE-driven luciferase activity and ERK1/2 phosphorylation. This suggests the essential role of Lys^{11} and Lys^{12} for NPS in activation of the Gα$_s$-dependent signaling pathway.

NPS and its receptor have been suggested to be involved in the regulation of a variety of aspects of central nervous system physiology and pathology, including those related to stress and anxiety, locomotor activity, wakefulness, food intake, and drug and alcohol abuse, all through Gα$_q$- and Gα$_s$-dependent pathways and the ERK1/2 signaling cascade (52). However, the contribution of individual G protein and ERK1/2 pathways to the diverse physiological responses mediated by NPS/NPSR remains unknown. One study (13) demonstrated that NCGC84, a novel small-molecule NPSR antagonist, showed biased antagonist properties, preferentially blocking ERK1/2 phosphorylation over cAMP accumulation and Ca^{2+} mobilization. Systemic pretreatment with NCGC84 resulted in the reduction of motivation for alcohol consumption (13). This suggests that the NPS/NPSR-mediated physiological effects may result from different signaling pathways. In addition, the human NPS-(1–10) has been found to fully mimic the *in vitro* effects of the full-length NPS in a Ca^{2+} mobilization assay but failed to induce a statistically significant effect on mouse locomotor activity *in vivo*, even using concentrations 100-fold higher than the first effective concentration of wild type NPS (8). The reason(s) for this *in vivo* failure may be attributed to the biased signaling properties of NPS-(1–10). The use of full-length NPS and NPS-(1–10) will be of great interest in additional *in vivo* behavioral and physiological models to evaluate the distribution of Gα$_q$- and Gα$_s$-dependent signaling. However, it will be important to assess whether or not the NPS-(1–10)-mediated biased signaling is associated with other physiological activities and behaviors.

In conclusion, we have demonstrated that the human NPS receptor elicits Gα$_q$-dependent Ca^{2+} mobilization, Gα$_s$-dependent CRE-driven luciferase activity, and both Gα$_q$- and Gα$_s$-dually coupled ERK1/2 phosphorylation in response to full-length human NPS. We provide strong evidence that at hNPSR, the NPS analog hNPS-(1–10) appears to be biased toward Gα$_q$-dependent Ca^{2+} mobilization and ERK1/2 activation and away from Gα$_s$-coupled CRE-driven luciferase activity and ERK1/2 phosphorylation. However, extensive future studies are required to further characterize the *in vivo* signaling profiles of the NPS receptor activated by NPS-(1–10) and to fully investigate how the different cellular signaling cascades induced by NPSR contribute to different *in vivo* physiological effects. This study brings new insights into the NPS receptor signaling mechanism and will be helpful to elucidate the NPSR-mediated

FIGURE 6. **hNPS-(1–13) analogs activate ERK1/2 via different signaling pathways in HEK293 cells.** Time course of PKA inhibitor H89 (10 μM) (*A*, *C*, *E*, and *F*) and Gα$_q$ inhibitor UBO-QIC (100 nM) (*B*, *D*, *G*, and *H*) on NPS variant-mediated activation of ERK1/2 in the following sequence: hNPS-K11A, hNPS-K12A, hNPS-T13A, hNPS-(1–13). The cells were pretreated with or without (control) inhibitors for 1 h and then stimulated with different hNPS variants (1 μM, 5 min). The phospho-ERK (*P-ERK*) was normalized to a loading control (total ERK (*T-ERK*)). The data shown are representative of at least three independent experiments. Statistical analysis was performed by a two-tailed Student's *t* test (*, $p < 0.05$; **, $p < 0.01$; ***, $p < 0.001$, *versus* counterpart control).

signaling pathways in both *in vitro* and, importantly, *in vivo* systems.

Author Contributions—N. Z. conceived and coordinated the study and wrote the paper. F. H. conceived the study. Y. L. designed, performed, and analyzed the experiments and contributed to the preparation of the figures and manuscript. B. L. and Q. M. performed and analyzed the experiments shown in Figs. 1 and 2. G. W., X. L., J. Z., and Y. S. performed and analyzed the experiments shown in Figs. 3, 4, and 6. D. L. designed mutant peptides. All authors reviewed the results and approved the final version of the manuscript.

Acknowledgments—We thank Aiping Shao, Ming Ding, and Hanmin Chen for technical assistance and use of equipment.

References

1. Xu, Y. L., Reinscheid, R. K., Huitron-Resendiz, S., Clark, S. D., Wang, Z., Lin, S. H., Brucher, F. A., Zeng, J., Ly, N. K., Henriksen, S. J., de Lecea, L., and Civelli, O. (2004) Neuropeptide S: a neuropeptide promoting arousal and anxiolytic-like effects. *Neuron* **43,** 487–497
2. Reinscheid, R. K. (2007) Phylogenetic appearance of neuropeptide S precursor proteins in tetrapods. *Peptides* **28,** 830–837
3. Sato S, S. Y., Miyajima N, Yoshimura K. (September 19, 2002) Novel G protein-coupled receptor protein and DNA thereof. International Patent Application WO2002072829 A1
4. Xu, Y. L., Gall, C. M., Jackson, V. R., Civelli, O., and Reinscheid, R. K. (2007) Distribution of neuropeptide S receptor mRNA and neurochemical characteristics of neuropeptide S-expressing neurons in the rat brain. *J. Comp. Neurol.* **500,** 84–102
5. Leonard, S. K., and Ring, R. H. (2011) Immunohistochemical localization of the neuropeptide S receptor in the rat central nervous system. *Neuroscience* **172,** 153–163
6. Rizzi, A., Vergura, R., Marzola, G., Ruzza, C., Guerrini, R., Salvadori, S., Regoli, D., and Calo, G. (2008) Neuropeptide S is a stimulatory anxiolytic agent: a behavioural study in mice. *Br. J. Pharmacol.* **154,** 471–479
7. Leonard, S. K., Dwyer, J. M., Sukoff Rizzo, S. J., Platt, B., Logue, S. F., Neal, S. J., Malberg, J. E., Beyer, C. E., Schechter, L. E., Rosenzweig-Lipson, S., and Ring, R. H. (2008) Pharmacology of neuropeptide S in mice: therapeutic relevance to anxiety disorders. *Psychopharmacology* **197,** 601–611
8. Roth, A. L., Marzola, E., Rizzi, A., Arduin, M., Trapella, C., Corti, C., Vergura, R., Martinelli, P., Salvadori, S., Regoli, D., Corsi, M., Cavanni, P., Caló, G., and Guerrini, R. (2006) Structure-activity studies on neuropeptide S: identification of the amino acid residues crucial for receptor activation. *J. Biol. Chem.* **281,** 20809–20816
9. Smith, K. L., Patterson, M., Dhillo, W. S., Patel, S. R., Semjonous, N. M., Gardiner, J. V., Ghatei, M. A., and Bloom, S. R. (2006) Neuropeptide S stimulates the hypothalamo-pituitary-adrenal axis and inhibits food intake. *Endocrinology* **147,** 3510–3518
10. Beck, B., Fernette, B., and Stricker-Krongrad, A. (2005) Peptide S is a novel potent inhibitor of voluntary and fast-induced food intake in rats. *Biochem. Biophys. Res. Commun.* **332,** 859–865
11. Han, R. W., Yin, X. Q., Chang, M., Peng, Y. L., Li, W., and Wang, R. (2009) Neuropeptide S facilitates spatial memory and mitigates spatial memory impairment induced by *N*-methyl-D-aspartate receptor antagonist in mice. *Neurosci. Lett.* **455,** 74–77
12. Badia-Elder, N. E., Henderson, A. N., Bertholomey, M. L., Dodge, N. C., and Stewart, R. B. (2008) The effects of neuropeptide S on ethanol drinking and other related behaviors in alcohol-preferring and -nonpreferring rats. *Alcohol. Clin. Exp. Res.* **32,** 1380–1387
13. Thorsell, A., Tapocik, J. D., Liu, K., Zook, M., Bell, L., Flanigan, M., Patnaik, S., Marugan, J., Damadzic, R., Dehdashti, S. J., Schwandt, M. L., Southall, N., Austin, C. P., Eskay, R., Ciccocioppo, R., *et al.* (2013) A novel brain penetrant NPS receptor antagonist, NCGC00185684, blocks alcohol-induced ERK-phosphorylation in the central amygdala and decreases operant alcohol self-administration in rats. *J. Neurosci.* **33,** 10132–10142
14. Meis, S., Bergado-Acosta, J. R., Yanagawa, Y., Obata, K., Stork, O., and Munsch, T. (2008) Identification of a neuropeptide S responsive circuitry shaping amygdala activity via the endopiriform nucleus. *PLoS One* **3,** e2695
15. Okamura, N., Garau, C., Duangdao, D. M., Clark, S. D., Jüngling, K., Pape, H. C., and Reinscheid, R. K. (2011) Neuropeptide S enhances memory during the consolidation phase and interacts with noradrenergic systems in the brain. *Neuropsychopharmacology* **36,** 744–752
16. Reinscheid, R. K., Xu, Y. L., Okamura, N., Zeng, J., Chung, S., Pai, R., Wang, Z., and Civelli, O. (2005) Pharmacological characterization of human and murine neuropeptide s receptor variants. *J. Pharmacol. Exp. Ther.* **315,** 1338–1345
17. Erdmann, F., Kügler, S., Blaesse, P., Lange, M. D., Skryabin, B. V., Pape, H. C., and Jüngling, K. (2015) Neuronal expression of the human neuropeptide S receptor NPSR1 identifies NPS-induced calcium signaling pathways. *PLoS One* **10,** e0117319
18. Pietras, C. O., Vendelin, J., Anedda, F., Bruce, S., Adner, M., Sundman, L., Pulkkinen, V., Alenius, H., D'Amato, M., Söderhall, C., and Kere, J. (2011) The asthma candidate gene NPSR1 mediates isoform specific downstream signalling. *BMC Pulm. Med.* **11,** 39
19. Bernier, V., Stocco, R., Bogusky, M. J., Joyce, J. G., Parachoniak, C., Grenier, K., Arget, M., Mathieu, M. C., O'Neill, G. P., Slipetz, D., Crackower, M. A., Tan, C. M., and Therien, A. G. (2006) Structure-function relationships in the neuropeptide S receptor: molecular consequences of the asthma-associated mutation N107I. *J. Biol. Chem.* **281,** 24704–24712
20. He, X., Zang, J., Yang, H., Huang, H., Shi, Y., Zhu, C., and Zhou, N. (2015) *Bombyx mori* prothoracicostatic peptide receptor is allosterically activated via a $G\alpha_{i/o}$-protein-biased signalling cascade by *Drosophila* sex peptide. *Biochem. J.* **466,** 391–400
21. Watts, A. O., van Lipzig, M. M., Jaeger, W. C., Seeber, R. M., van Zwam, M., Vinet, J., van der Lee, M. M., Siderius, M., Zaman, G. J., Boddeke, H. W., Smit, M. J., Pfleger, K. D., Leurs, R., and Vischer, H. F. (2013) Identification and profiling of CXCR3-CXCR4 chemokine receptor heteromer complexes. *Br. J. Pharmacol.* **168,** 1662–1674
22. Lee, H. Y., Kim, S. D., Shim, J. W., Kim, H. J., Kwon, J. Y., Kim, J. M., Baek, S. H., Park, J. S., and Bae, Y. S. (2010) Activation of human monocytes by a formyl peptide receptor 2-derived pepducin. *FEBS Lett.* **584,** 4102–4108
23. Sroussi, H. Y., Lu, Y., Villines, D., and Sun, Y. (2012) The down regulation of neutrophil oxidative metabolism by S100A8 and S100A9: implication of the protease-activated receptor-2. *Mol. Immunol.* **50,** 42–48
24. Black, J. W., and Leff, P. (1983) Operational models of pharmacological agonism. *Proc. R. Soc. Lond. B Biol. Sci.* **220,** 141–162
25. van der Westhuizen, E. T., Breton, B., Christopoulos, A., and Bouvier, M. (2014) Quantification of ligand bias for clinically relevant β_2-adrenergic receptor ligands: implications for drug taxonomy. *Mol. Pharmacol.* **85,** 492–509
26. Jacobsen, S. E., Nørskov-Lauritsen, L., Thomsen, A. R., Smajilovic, S., Wellendorph, P., Larsson, N. H., Lehmann, A., Bhatia, V. K., and Bräuner-Osborne, H. (2013) Delineation of the GPRC6A receptor signaling pathways using a mammalian cell line stably expressing the receptor. *J. Pharmacol. Exp. Ther.* **347,** 298–309
27. Figueroa, K. W., Griffin, M. T., and Ehlert, F. J. (2009) Selectivity of agonists for the active state of M1 to M4 muscarinic receptor subtypes. *J. Pharmacol. Exp. Ther.* **328,** 331–342
28. Ceraudo, E., Galanth, C., Carpentier, E., Banegas-Font, I., Schonegge, A. M., Alvear-Perez, R., Iturrioz, X., Bouvier, M., and Llorens-Cortes, C. (2014) Biased signaling favoring G_i over β-arrestin promoted by an apelin fragment lacking the C-terminal phenylalanine. *J. Biol. Chem.* **289,** 24599–24610
29. Lee, M. H., El-Shewy, H. M., Luttrell, D. K., and Luttrell, L. M. (2008) Role of β-arrestin-mediated desensitization and signaling in the control of angiotensin AT1a receptor-stimulated transcription. *J. Biol. Chem.* **283,** 2088–2097
30. Chen, Z., Gibson, T. B., Robinson, F., Silvestro, L., Pearson, G., Xu, B., Wright, A., Vanderbilt, C., and Cobb, M. H. (2001) MAP kinases. *Chem. Rev.* **101,** 2449–2476
31. Clark, S. D., Tran, H. T., Zeng, J., and Reinscheid, R. K. (2010) Importance of extracellular loop one of the neuropeptide S receptor for biogenesis and

function. *Peptides* **31,** 130–138
32. Anedda, F., Zucchelli, M., Schepis, D., Hellquist, A., Corrado, L., D'Alfonso, S., Achour, A., McInerney, G., Bertorello, A., Lördal, M., Befrits, R., Björk, J., Bresso, F., Törkvist, L., Halfvarson, J., *et al.* (2011) Multiple polymorphisms affect expression and function of the neuropeptide S receptor (NPSR1). *PLoS One* **6,** e29523
33. Karpinsky-Semper, D., Volmar, C. H., Brothers, S. P., and Slepak, V. Z. (2014) Differential effects of the Gβ5-RGS7 complex on muscarinic M3 receptor-induced Ca^{2+} influx and release. *Mol. Pharmacol.* **85,** 758–768
34. Gregory, K. J., Hall, N. E., Tobin, A. B., Sexton, P. M., and Christopoulos, A. (2010) Identification of orthosteric and allosteric site mutations in M2 muscarinic acetylcholine receptors that contribute to ligand-selective signaling bias. *J. Biol. Chem.* **285,** 7459–7474
35. Urban, J. D., Clarke, W. P., von Zastrow, M., Nichols, D. E., Kobilka, B., Weinstein, H., Javitch, J. A., Roth, B. L., Christopoulos, A., Sexton, P. M., Miller, K. J., Spedding, M., and Mailman, R. B. (2007) Functional selectivity and classical concepts of quantitative pharmacology. *J. Pharmacol. Exp. Ther.* **320,** 1–13
36. Rajagopal, S., Rajagopal, K., and Lefkowitz, R. J. (2010) Teaching old receptors new tricks: biasing seven-transmembrane receptors. *Nat. Rev. Drug Discov.* **9,** 373–386
37. Patel, C. B., Noor, N., and Rockman, H. A. (2010) Functional selectivity in adrenergic and angiotensin signaling systems. *Mol. Pharmacol.* **78,** 983–992
38. Mottola, D. M., Kilts, J. D., Lewis, M. M., Connery, H. S., Walker, Q. D., Jones, S. R., Booth, R. G., Hyslop, D. K., Piercey, M., Wightman, R. M., Lawler, C. P., Nichols, D. E., and Mailman, R. B. (2002) Functional selectivity of dopamine receptor agonists. I. Selective activation of postsynaptic dopamine D2 receptors linked to adenylate cyclase. *J. Pharmacol. Exp. Ther.* **301,** 1166–1178
39. Gesty-Palmer, D., Chen, M., Reiter, E., Ahn, S., Nelson, C. D., Wang, S., Eckhardt, A. E., Cowan, C. L., Spurney, R. F., Luttrell, L. M., and Lefkowitz, R. J. (2006) Distinct β-arrestin- and G protein-dependent pathways for parathyroid hormone receptor-stimulated ERK1/2 activation. *J. Biol. Chem.* **281,** 10856–10864
40. Gesty-Palmer, D., Flannery, P., Yuan, L., Corsino, L., Spurney, R., Lefkowitz, R. J., and Luttrell, L. M. (2009) A β-arrestin-biased agonist of the parathyroid hormone receptor (PTH1R) promotes bone formation independent of G protein activation. *Sci. Transl. Med.* **1,** 1ra1
41. Maudsley, S., Martin, B., Gesty-Palmer, D., Cheung, H., Johnson, C., Patel, S., Becker, K. G., Wood, W. H., 3rd, Zhang, Y., Lehrmann, E., and Luttrell, L. M. (2015) Delineation of a conserved arrestin-biased signaling repertoire in vivo. *Mol. Pharmacol.* **87,** 706–717
42. Brulé, C., Perzo, N., Joubert, J. E., Sainsily, X., Leduc, R., Castel, H., and Prézeau, L. (2014) Biased signaling regulates the pleiotropic effects of the urotensin II receptor to modulate its cellular behaviors. *FASEB J.* **28,** 5148–5162
43. Charest, P. G., Oligny-Longpré, G., Bonin, H., Azzi, M., and Bouvier, M. (2007) The V2 vasopressin receptor stimulates ERK1/2 activity independently of heterotrimeric G protein signalling. *Cell. Signal.* **19,** 32–41
44. Watson, S. J., Brown, A. J., and Holliday, N. D. (2012) Differential signaling by splice variants of the human free fatty acid receptor GPR120. *Mol. Pharmacol.* **81,** 631–642
45. Sbai, O., Monnier, C., Dodé, C., Pin, J. P., Hardelin, J. P., and Rondard, P. (2014) Biased signaling through G-protein-coupled PROKR2 receptors harboring missense mutations. *FASEB J.* **28,** 3734–3744
46. Corbisier, J., Galès, C., Huszagh, A., Parmentier, M., and Springael, J. Y. (2015) Biased signaling at chemokine receptors. *J. Biol. Chem.* **290,** 9542–9554
47. Davey, A. E., Leach, K., Valant, C., Conigrave, A. D., Sexton, P. M., and Christopoulos, A. (2012) Positive and negative allosteric modulators promote biased signaling at the calcium-sensing receptor. *Endocrinology* **153,** 1232–1241
48. Makita, N., Sato, J., Manaka, K., Shoji, Y., Oishi, A., Hashimoto, M., Fujita, T., and Iiri, T. (2007) An acquired hypocalciuric hypercalcemia autoantibody induces allosteric transition among active human Ca-sensing receptor conformations. *Proc. Natl. Acad. Sci. U.S.A.* **104,** 5443–5448
49. Alonso, N., Monczor, F., Echeverría, E., Davio, C., Shayo, C., and Fernández, N. (2014) Signal transduction mechanism of biased ligands at histamine H2 receptors. *Biochem. J.* **459,** 117–126
50. Busnelli, M., Saulière, A., Manning, M., Bouvier, M., Galés, C., and Chini, B. (2012) Functional selective oxytocin-derived agonists discriminate between individual G protein family subtypes. *J. Biol. Chem.* **287,** 3617–3629
51. Arey, B. J., and López, F. J. (2011) Are circulating gonadotropin isoforms naturally occurring biased agonists? Basic and therapeutic implications. *Rev. Endocr. Metab. Disord.* **12,** 275–288
52. Guerrini, R., Salvadori, S., Rizzi, A., Regoli, D., and Calo', G. (2010) Neurobiology, pharmacology, and medicinal chemistry of neuropeptide S and its receptor. *Med. Res. Rev.* **30,** 751–777